Appendix A.23:

Normans Rd/Papanui Rd – VsVp 57200

Table 1: Site Description for Normans Rd/Papanui Rd (VsVp 57200).

Attribute	Yes/No			Description/Date	Symbol in Figure 1
	10-m Buffer	20-m Buffer	50-m Buffer		
Near a body of surface water or other free face features?	No	No	Yes	The center of the site is 20 m away from an unnamed stream running through the SE and SW quadrants. The direction of the free face is roughly NE-SW, while its height is ~1.5 m.	NA
Lateral spreading observed during the CES?	No	No	No	No lateral spreading was observed for the September 2010 earthquake but the February 2011 earthquake. [1,*]	NA
Nearby buildings or structures?	No	No	Yes	Building coverage of the 50-m buffer is 9%. The structures are in the NW and NE quadrants.	White Fill + Brown Outline
Sloping land?	No	No	Yes	Predominantly flat, residential area; however, there is a slightly sloping ground toward and along the stream in the S portion of the 50-m buffer.	NA
Step changes in the ground surface?	No	No	Yes	Along the stream.	NA
Retaining walls?	No	No	No	NA	NA
Vegetation?	Yes	Yes	Yes	Trees and bushes cover 76, 65, and 46% of the 10-, 20-, and 50-m buffers, respectively. They are in all quadrants of the buffers.	White Fill + Green Outline
Anthropogenic changes to the site between the LiDAR surveys?	No	No	Yes	Building construction, removal, and addition of vegetation in the NW quadrant of the 50-m buffer between Jun 2009 and Sep 2010. Traffic island construction on Normans Rd at the intersection with Papanui Rd between Jun 2006 and Sep 2010.	Building Addition: Yellow Outline; Vegetation Removal: Green Crossline; Vegetation Addition: Green Outline; Island Addition: Orange Outline
Other important factors?	Yes	Yes	Yes	Two roads occupy 4, 23, and 24% of the 10-, 20-, and 50-m buffers, respectively and stretch through all quadrants.	Outline Road: Gray Fill + Red Outline (excludes vegetation)

Notes: Buffer is the area within a circle of a specified radius with CPT investigations done at its center (172.615699°, -43.506100°); * indicates that the settlement analysis was conducted only for the September 2011 earthquake due to the lateral spreading observed for the February 2011 earthquake (the anthropogenic changes description pertains to the period between Dec 2004 and Feb 2011 only).

[1] Canterbury Geotechnical Database. (2012). "Observed Ground Crack Locations", Map Layer CGD0400 - 23 July 2012, retrieved July 09, 2018 from https://canterburygeotechnicaldatabase.projectorbit.com/

Figure 1: Site plan with areas where ejecta-induced settlement is considered.

Note 1: Road (outlined in red) is the only area selected for detailed settlement assessment because most of the site is covered with vegetation and buildings or was subjected to the addition of a structure and/or front yard/backyard alterations (e.g., addition or removal of vegetation). However, the LiDAR-based settlement analysis was not performed due to the evident absence of ejecta for the Sep-10 EQ. Also, the site was not assessed for the ejecta-induced settlement for the Feb-11, Jun-11, and Dec-11 EQs due to lateral spreading.

Table 2: LiDAR flight error adjustments, global adjustments for the difference between average LiDAR point elevations and benchmark survey elevations, and vertical tectonic movement adjustments.

	Adjustments (mm)		
Earthquake Event(s)	LiDAR Flight Error	Global Offset[2]	Tectonic Vertical Movement
Sep-10	-50	-3	0
Feb-11	+50	16	-50
Jun-11	0	38	-25
Dec-11	-50	-65	0
CES	-50	-14	-75
Any LiDAR survey affected by ejecta?			No

Note: The negative sign indicates the subtraction from the ground surface subsidence, while the positive sign indicates the addition to the ground surface subsidence.

Table 3: LiDAR Measurement Error for Road.

Surveys	Buffer	Area Averaged Difference Indicating Repeat Measurement Error (mm)	$\sigma^*_{\text{individual LiDAR points}}$ (mm)	%Reduction in σ due to Area Averaging of LiDAR Points
Post Feb 2011: Mar 2011 and May 2011	10-m	ND	59	[ND,ND]
	20-m	ND		
	50-m	ND		
Post Dec 2011: Feb 2012 and Oct 2015	10-m	ND	70	[ND,ND]
	20-m	ND		
	50-m	ND		

*Standard deviation; ND = Not determined.

[2] Russell, J., & van Ballegooy, S. (2015). *Canterbury Earthquake Sequence: Increased liquefaction vulnerability assessment methodology*. New Zealand: Tonkin & Taylor Ltd.

Table 4: Ground surface subsidence adjustments due to LiDAR measurement error for Road.

Earthquake Event(s)	$\sigma_{\text{pre-EQ LiDAR survey}}$ (mm)	$\sigma_{\text{post-EQ LiDAR survey}}$ (mm)	σ_{total} (mm)	Area Average Adjusted σ (mm) **
Sep-10	158	56	134	ND
Feb-11	56	59	59	ND
Jun-11	59	61	62	ND
Dec-11	61	70	87	ND
CES	158	70	124	ND

**Based on the highest %Reduction in Table 3a; ND = Not determined.

Table 5: Raw liquefaction-related ground surface subsidence using original LiDAR points for Road.

	Average Ground Surface Subsidence (mm)		
Earthquake Event(s)	10-m Buffer	20-m Buffer	50-m Buffer
Sep-10	ND	ND	ND
Feb-11	ND	ND	ND
Jun-11	ND	ND	ND
Dec-11	ND	ND	ND
CES	ND	ND	ND

Notes: NA = Not available; ND = Not determined.

Table 6: Corrected liquefaction-related ground surface subsidence using original LiDAR points for Road with the calculated adjustments in Table 2.

	Average Calculated Ground Surface Subsidence (mm)		
Earthquake Event(s)	10-m Buffer	20-m Buffer	50-m Buffer
Sep-10	NA	ND	ND
Feb-11	NA	ND	ND
Jun-11	NA	ND	ND
Dec-11	NA	ND	ND
CES	NA	ND	ND

Notes: Plus/minus values are same as those in Table 4a, but rounded to the nearest 25; Positive overall values indicate ground surface subsidence, while negative overall values indicate ground surface uplift; NA = Not available; ND = Not determined.

Table 7: Corrected liquefaction-related ground surface subsidence for Road using LiDAR DEMs.

	Estimated Ground Surface Subsidence (mm)								
	10-m Buffer			20-m Buffer			50-m Buffer		
Earthquake Event(s)	16^{th} %ile	50^{th} %ile	84^{th} %ile	16^{th} %ile	50^{th} %ile	84^{th} %ile	16^{th} %ile	50^{th} %ile	84^{th} %ile
Sep-10	NA	NA	NA	<50	50	100	<50	50	100
Feb-11	ND	ND	ND	ND	ND	ND	ND	ND	ND
Jun-11	ND	ND	ND	ND	ND	ND	ND	ND	ND
Dec-11	ND	ND	ND	ND	ND	ND	ND	ND	ND
CES	ND	ND	ND	ND	ND	ND	ND	ND	ND

Note: These percentiles are not the exact statistical measures; they indicate the spatial variability of ground surface subsidence; ND = Not determined.

Table 8a: Ejecta-Induced settlement for the top 20 m of the soil profile for Road (20-m buffer) for the 50th %ile PGA, P_L=50%, and C_{FC}=0.13 using BI-2014, ZRB-2002, and I_C cutoff of 2.6.

Earthquake Event(s)	M_W	PGA (g)	Depth to Groundwater (m)	S_T (mm)	S_{V1D} (mm)	$S_{E,L}$ (mm)
Sep-10	7.1	0.21	2.4	ND	47±20	ND
Feb-11	6.2	0.31	2.5	ND	ND	ND
Jun-11	6.2	0.17	1.8	ND	ND	ND
Dec-11	6.1	0.18	2.1	ND	ND	ND

Notes: S_T = Total settlement (Table 6); S_{V1D} = Average vertical settlement due to volumetric compression using Boulanger and Idriss (2014) (BI-2014), Zhang et al. (2002) (ZRB-2002) procedures and de Greef and Lengkeek (2018) thin-layer correction; $S_{E,L}$ = Ejecta-induced settlement as the difference between the LiDAR-based S_T and S_{V1D}.

Table 8b: Ejecta-Induced settlement for the top 20 m of the soil profile for Road (50-m buffer) for the 50th %ile PGA, P_L=50%, and C_{FC}=0.13 using BI-2014, ZRB-2002, and I_C cutoff of 2.6.

Earthquake Event(s)	M_W	PGA (g)	Depth to Groundwater (m)	S_T (mm)	S_{V1D} (mm)	$S_{E,L}$ (mm)
Sep-10	7.1	0.21	2.4	ND	64±20	ND
Feb-11	6.2	0.31	2.5	ND	ND	ND
Jun-11	6.2	0.17	1.8	ND	ND	ND
Dec-11	6.1	0.18	2.1	ND	ND	ND

Notes: S_T = Total settlement (Table 6); S_{V1D} = Average vertical settlement due to volumetric compression using Boulanger and Idriss (2014) (BI-2014), Zhang et al. (2002) (ZRB-2002) procedures and de Greef and Lengkeek (2018) thin-layer correction; $S_{E,L}$ = Ejecta-induced settlement as the difference between the LiDAR-based S_T and S_{V1D}.

Note 2: The uncertainty for volumetric settlement was derived based on the sensitivity of volumetric settlement to PGA, C_{FC}, and P_L for each earthquake event for VsVp 57203 *Shirley Intermediate School* and CC LIQ 1 – CPT 5586 – *Vivian St* sites. Taking the 50th percentile as the baseline case, the minimum and maximum values corresponding to the difference between the 25th percentile and the 50th percentile and the 75th percentile and the 50th percentile were determined. The arithmetic mean of the range of the minimum and maximum difference was evaluated for each patch at the two sites. The maximum arithmetic mean for each earthquake event was rounded to the nearest five and used as the uncertainty value. Accordingly, the 1-D volumetric settlement uncertainties of ±20, ±50, ±25, and ±50 mm for the Sep-10, Feb-11, Jun-11, and Dec-11 earthquake events, respectively, were used for all sites in this study.

Table 9a: Coverage area and height of ejecta estimates for Road (20-m buffer) using photographs.

Earthquake Event	$A_{E,thick}$ (m²)	$H_{E,thick}$ (mm)	$A_{E,thin}$ (m²)	$H_{E,thin}$ (mm)	A_T (m²)
Sep-10	0	0	0	0	272
Feb-11	ND	ND	ND	ND	272
Jun-11	ND	ND	ND	ND	272
Dec-11	ND	ND	ND	ND	272

Notes: $A_{E,thick/thin}$ = Coverage area of thick/thin ejecta layers; $H_{E,thick/thin}$ = Lower-upper estimate of height of thick/thin ejecta layers; A_T = Total assessment area of a buffer being considered; Thin and thick layers correspond to light gray and dark gray colors of ejecta observed in aerial photographs; ND = Not determined due to lateral spreading.

Table 9b: Coverage area and height of ejecta estimates for Road (50-m buffer) using photographs.

Earthquake Event	$A_{E,thick}$ (m²)	$H_{E,thick}$ (mm)	$A_{E,thin}$ (m²)	$H_{E,thin}$ (mm)	A_T (m²)
Sep-10	0	0	0	0	1765
Feb-11	ND	ND	ND	ND	1765
Jun-11	ND	ND	ND	ND	1765
Dec-11	ND	ND	ND	ND	1765

Notes: $A_{E,thick/thin}$ = Coverage area of thick/thin ejecta layers; $H_{E,thick/thin}$ = Lower-upper estimate of height of thick/thin ejecta layers; A_T = Total assessment area of a buffer being considered; Thin and thick layers correspond to light gray and dark gray colors of ejecta observed in aerial photographs; ND = Not determined due to lateral spreading.

Note 3: The values in Table 9 are based on satellite and aerial photographs (Figures 8, 9, and 11). The ejecta-induced settlement using photographs and engineering judgment, $S_{E,P}$, is estimated as

$$S_{E,P} = \frac{\sum_{i=1}^{a} A_{E,thick,i} * H_{E,thick,i} + \sum_{j=1}^{b} A_{E,thin,j} * H_{E,thin,j}}{A_T} = \frac{\sum_{i=1}^{a} V_{E,thick,i} + \sum_{j=1}^{b} V_{E,thin,j}}{A_T}$$

where

- $A_{E,thick,i}$ and $H_{E,thick,i}$ are the area and the height of a thick ejecta layer, respectively;
- $A_{E,thin,j}$ and $H_{E,thin,j}$ are the area and the height of a thin ejecta layer, respectively;
- A_T is the total assessment area for a buffer being considered (Figure 1).

Table 10: Ejecta-induced settlement estimates for Road (20-m and 50-m buffers) based on photographs.

Earthquake Event	Road (20-m buffer)		Road (50-m buffer)	
	$S_{E,P,lower}$ (mm)	$S_{E,P,upper}$ (mm)	$S_{E,P,lower}$ (mm)	$S_{E,P,upper}$ (mm)
Sep-10	0	0	0	0
Feb-11	ND	ND	ND	ND
Jun-11	ND	ND	ND	ND
Dec-11	ND	ND	ND	ND

Notes: $S_{E,P,lower}$ and $S_{E,P,upper}$ correspond to lower and upper estimates of $S_{E,P}$, respectively; ND = Not determined.

Table 11: Best final estimates of ejecta-induced settlement for Road (20-m and 50-m buffers).

Earthquake Event	Road (20-m buffer)			Road (50-m buffer)		
	$S_{E,L}$ (mm)	$S_{E,P}$ (mm)	$S_{E,final}$ (mm)	$S_{E,L}$ (mm)	$S_{E,P}$ (mm)	$S_{E,final}$ (mm)
Sep-10	ND	0	0	ND	0	0
Feb-11	ND	ND	ND	ND	ND	ND
Jun-11	ND	ND	ND	ND	ND	ND
Dec-11	ND	ND	ND	ND	ND	ND

Notes: $S_{E,L}$ = Ejecta-induced settlement based on LiDAR data reported in Table 8; $S_{E,P}$ = Median ejecta-induced settlement for the range of values reported in Table 10; $S_{E,final}$ = Best final estimate of ejecta-induced settlement rounded to the nearest 5; Final plus/minus values are also rounded to the nearest 5; ND = Not determined.

Note 4:

- $S_{E,final}$ for Road is based solely on $S_{E,P}$ for the Sep-10 earthquake due to the evident absence of ejecta.
- The site is in the zone of moderate to severe LPI overprediction of liquefaction severity for the Sep-10 EQ and moderate LPI overprediction of liquefaction severity for the Feb-11 EQ (Maurer et al. 2014[3]).

Summary:

The best estimate of the ejecta-induced free-field ground settlement at the Normans Rd/Papanui Rd site for the SEP 2010 earthquake is 0 mm. The free-field ground settlement was not assessed for the FEB 2011, JUN 2011, and DEC 2011 earthquakes due to lateral spreading.

[3] Maurer, B. W., Green, R. A., Cubrinovski, M., & Bradley, B. A. (2014). Evaluation of the Liquefaction Potential Index for Assessing Liquefaction Hazard in Christchurch, New Zealand. *Journal of Geotechnical and Geoenvironmental Engineering*, 140(7), 04014032-1-11. doi:10.1061/(asce)gt.1943-5606.0001117

Figure 2: Location of the site.

Figure 3: Position of the site relative to nearby buildings, vegetation, and free-face features.

Figure 4: Street view of the site.

Figure 5: Satellite image of the site taken in Apr 2004.

Figure 6: Satellite image of the site taken in Mar 2009.

Figure 7: Satellite image of the site taken in Jun 2009.

Figure 8: Satellite image of the site taken on Sep 3, 2010.

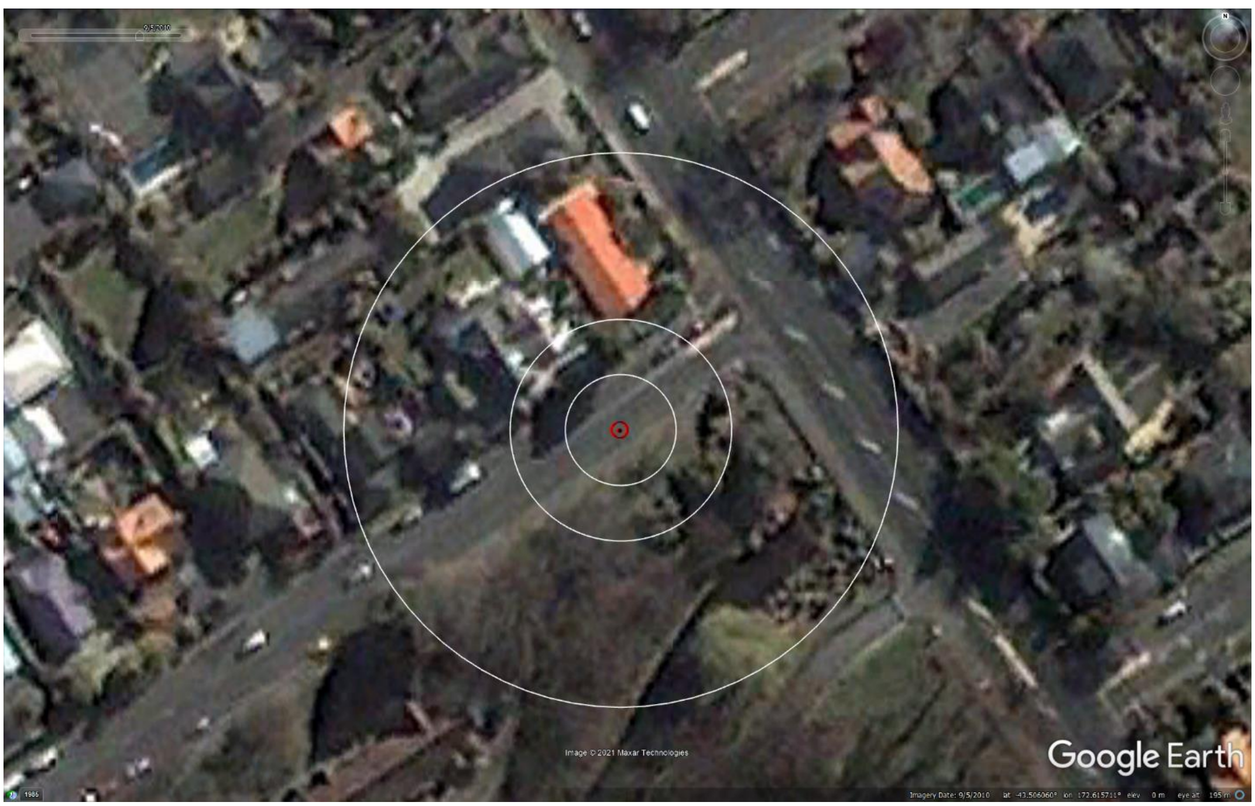

Figure 9: Satellite image of the site taken on Sep 5, 2010.

Figure 10: Satellite image of the site taken on Feb 7, 2011.

Figure 11: Aerial photograph of the site taken on Sep 4, 2010.

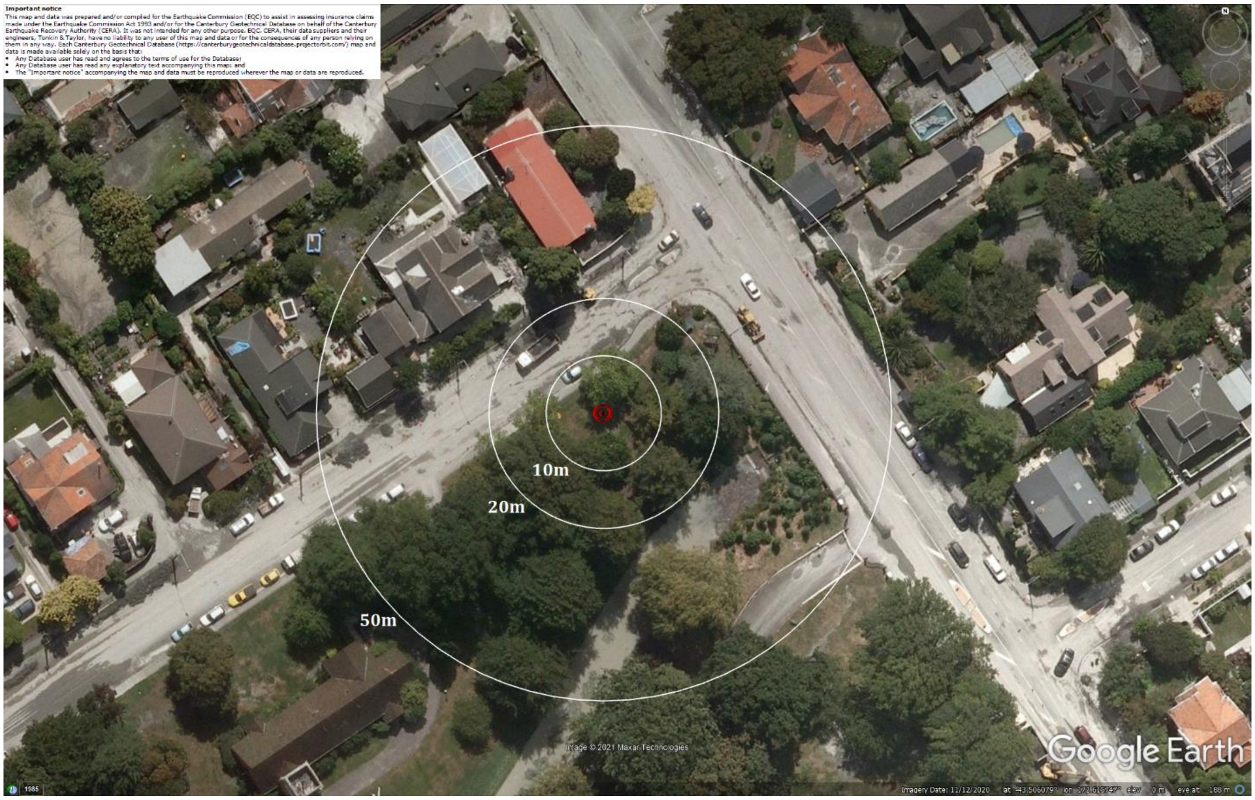

Figure 12: Aerial photograph of the site taken on Feb 24, 2011.

Figure 13: Aerial photograph of the site taken on June 14-15, 2011.

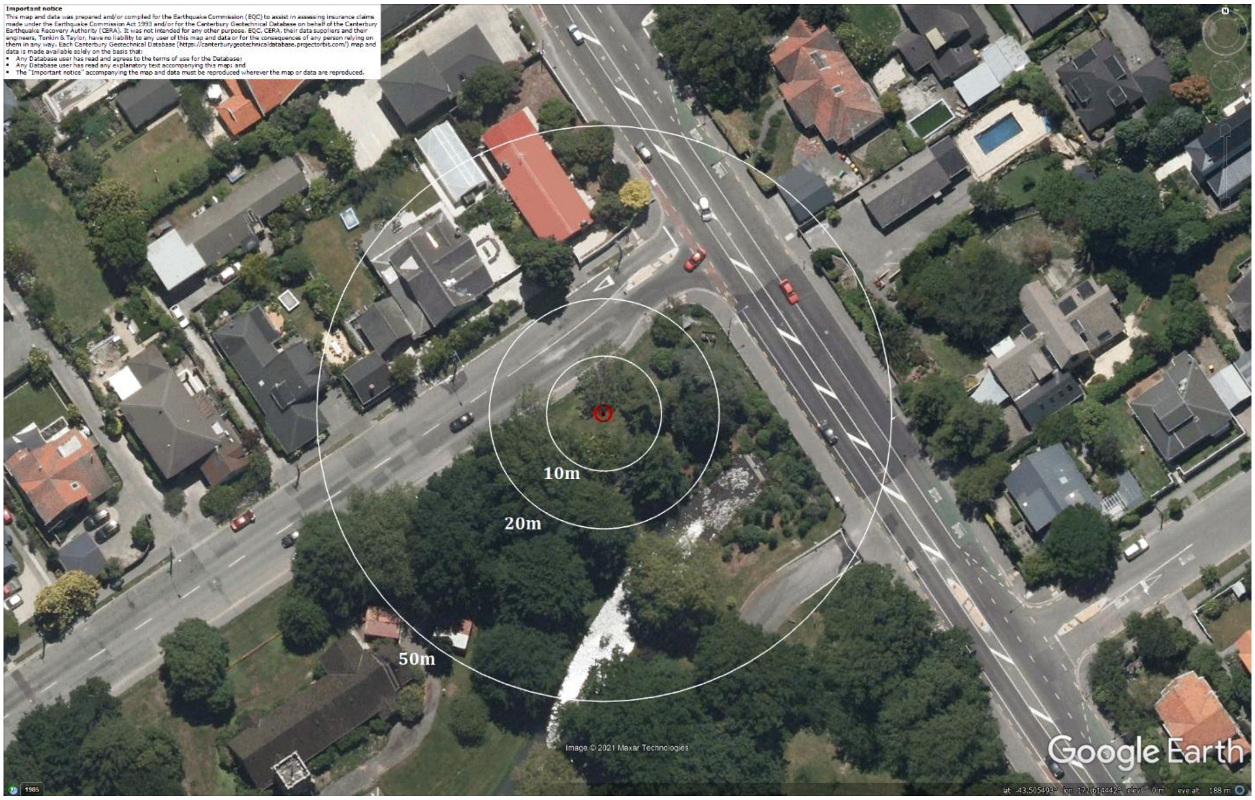

Figure 14: Aerial photograph of the site taken on Dec 24, 2011.

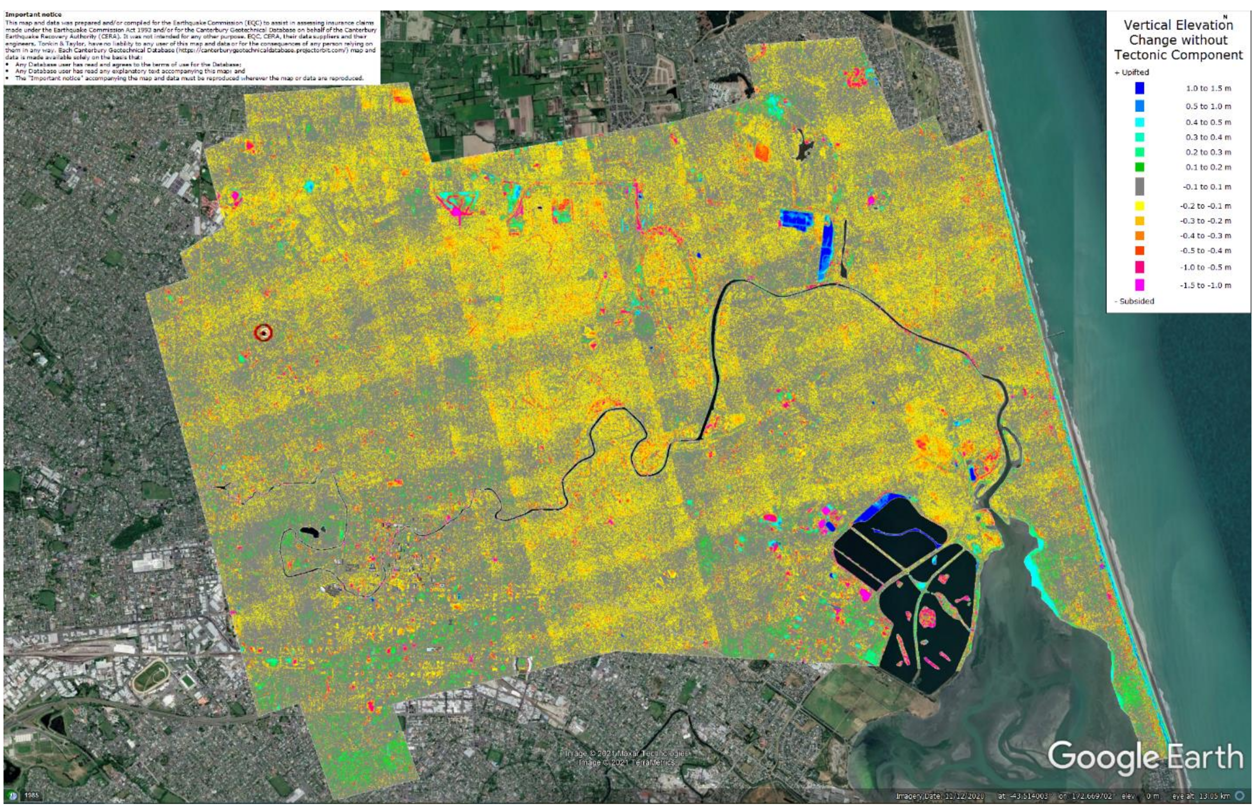

Figure 15: Vertical Ground Movements (Surface – Tectonic) for Sep 2010 Earthquake – the

site is in the apparent zone of overestimated ground surface subsidence (i.e., flight error band for Sep 2010).

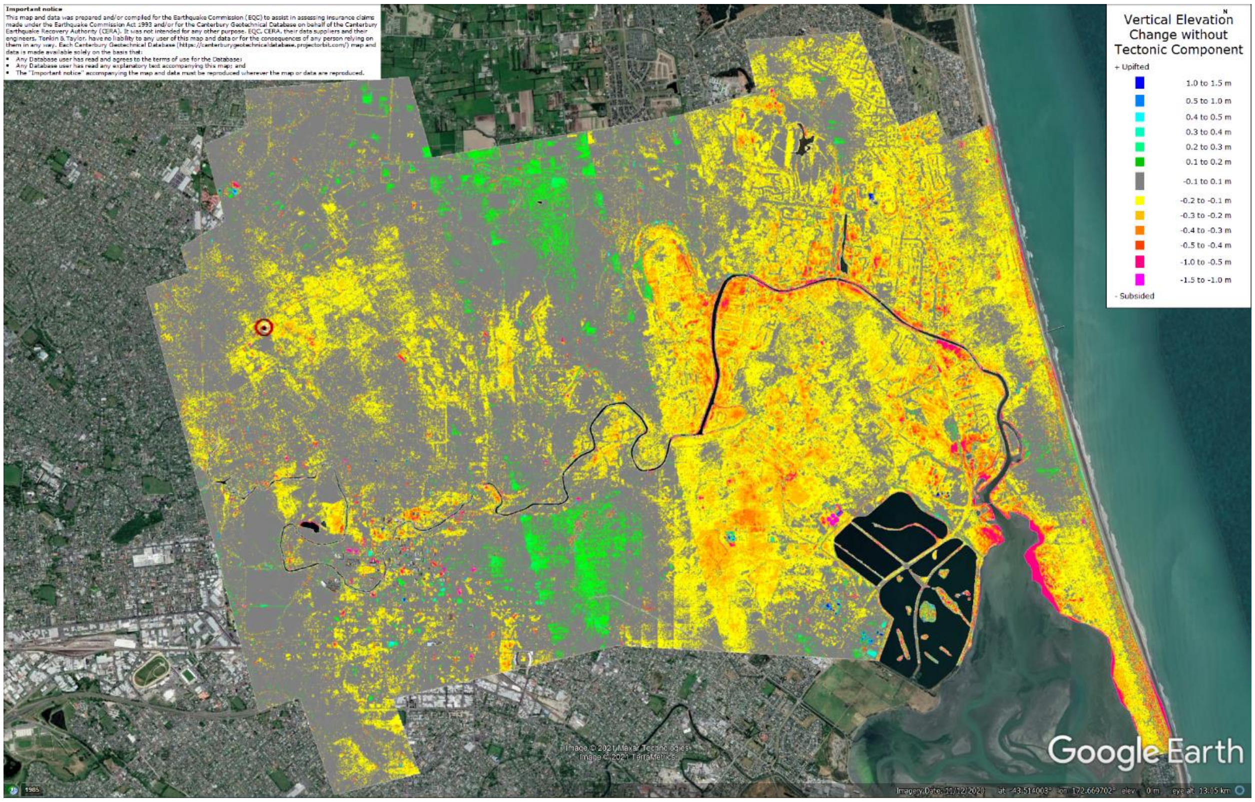

Figure 16: Vertical Ground Movements (Surface – Tectonic) for Feb 2011 Earthquake – the site is in the apparent zone of underestimated ground surface subsidence (i.e., flight error band for Sep 10).

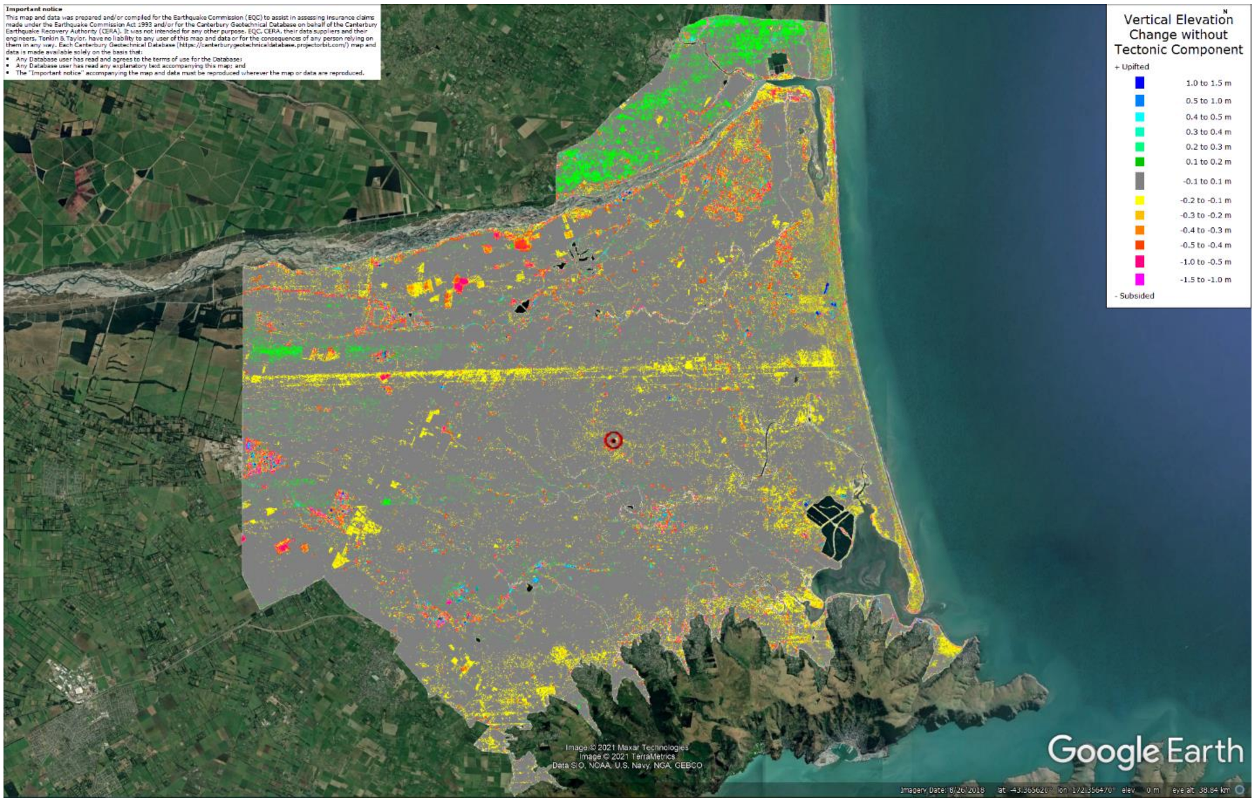

Figure 17: Vertical Ground Movements (Surface – Tectonic) for June 2011 Earthquake – the site is not in the apparent zone of overestimated ground surface subsidence.

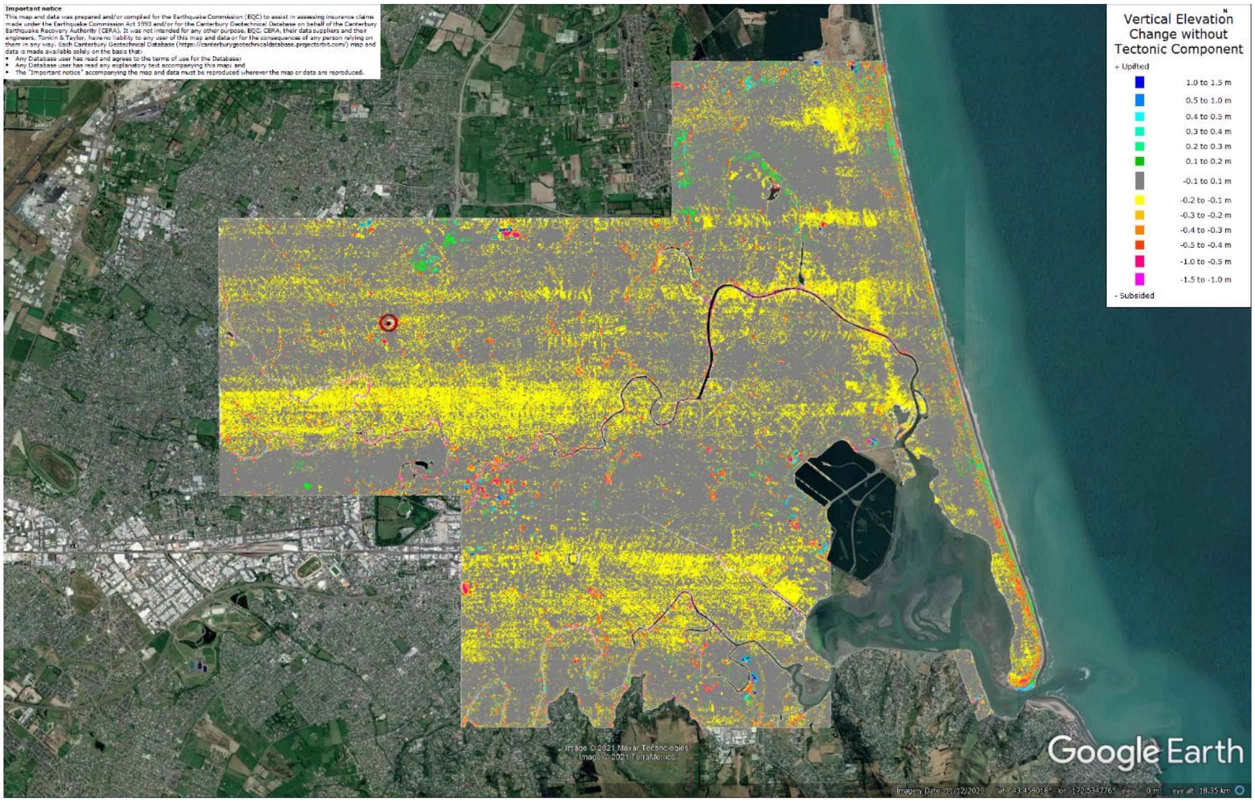

Figure 18: Vertical Ground Movements (Surface – Tectonic) for Dec 2011 Earthquake – the site is in the apparent zone of overestimated ground surface subsidence (i.e., flight error band for Feb 2012).

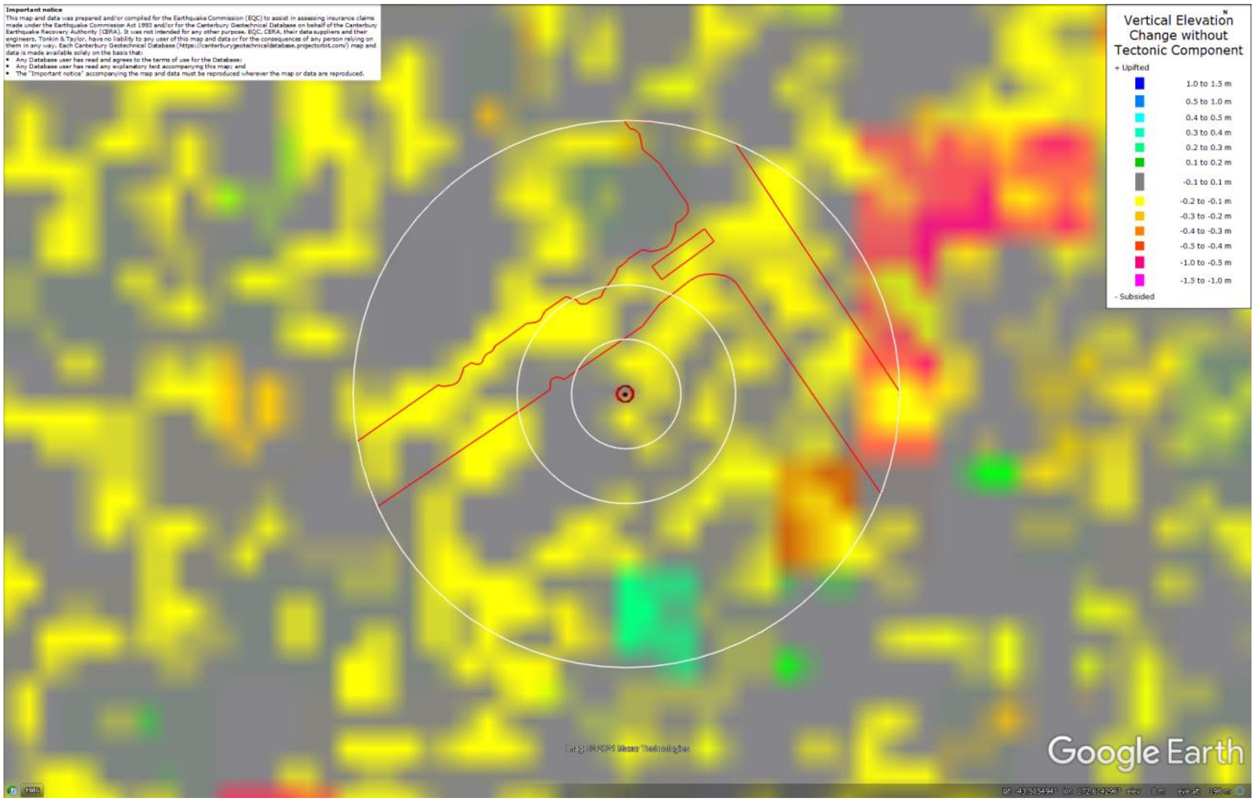

Figure 19: Ground surface subsidence without tectonic component for Sep 2010 Earthquake according to the LiDAR DEM.

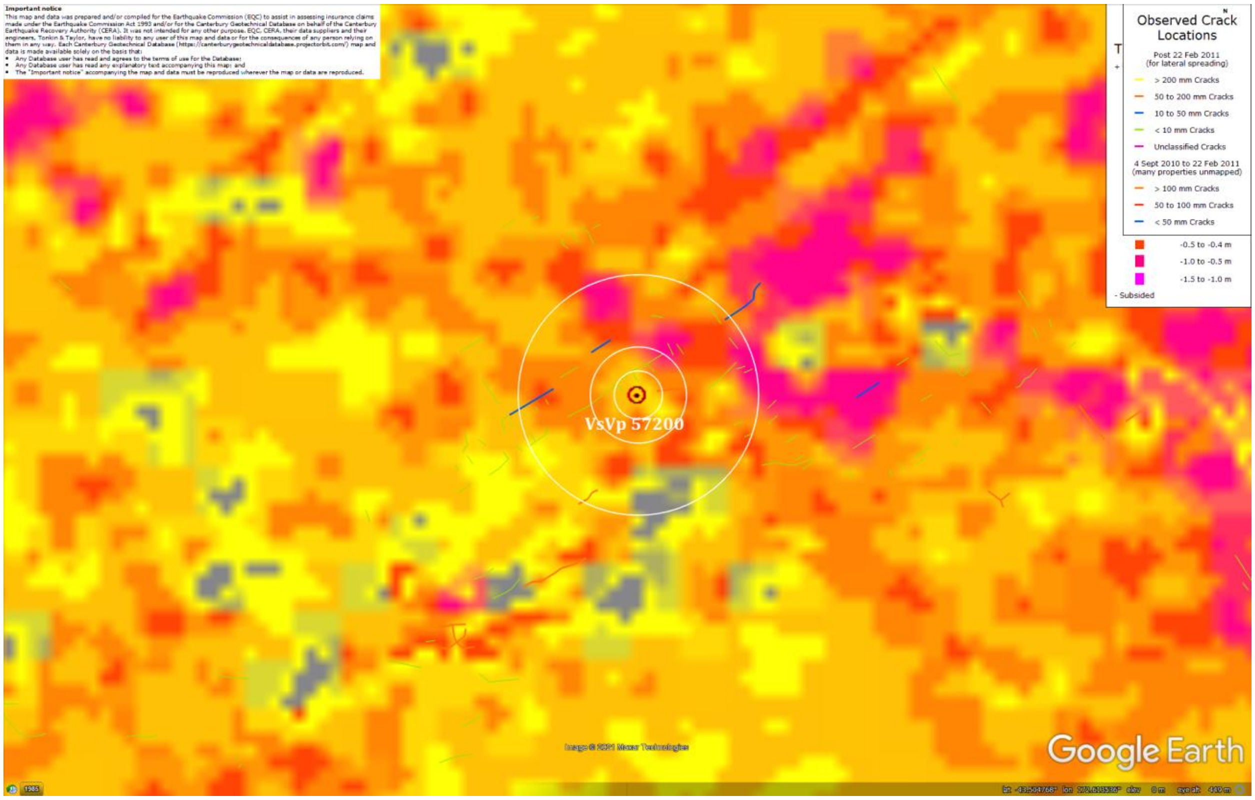

Figure 20: Cracks indicating lateral spreading for Canterbury Earthquake Sequence (no lateral spreading was observed for the Sep 2010 Earthquake).

Figure 21: Vertical tectonic movements for Sep 2010 Earthquake.

Figure 22: Vertical tectonic movements for Feb 2011 Earthquake.

Figure 23: Vertical tectonic movements for June 2011 Earthquake.

Figure 24: Vertical tectonic movements for Dec 2011 Earthquake.

Figure 25: Vertical tectonic movements for Canterbury Earthquake Sequence.

Figure 26: PGA for Sep-10 EQ (st. dev. = 0.300-0.325 ln units).

Figure 27: PGA for Feb-11 EQ (st. dev. = 0.350-0.375 ln units).

Figure 28: PGA for Jun-11 EQ (st. dev. = 0.350-0.375 ln units).

Figure 29: PGA for Dec-11 EQ (st. dev. = 0.375-0.400 ln units).

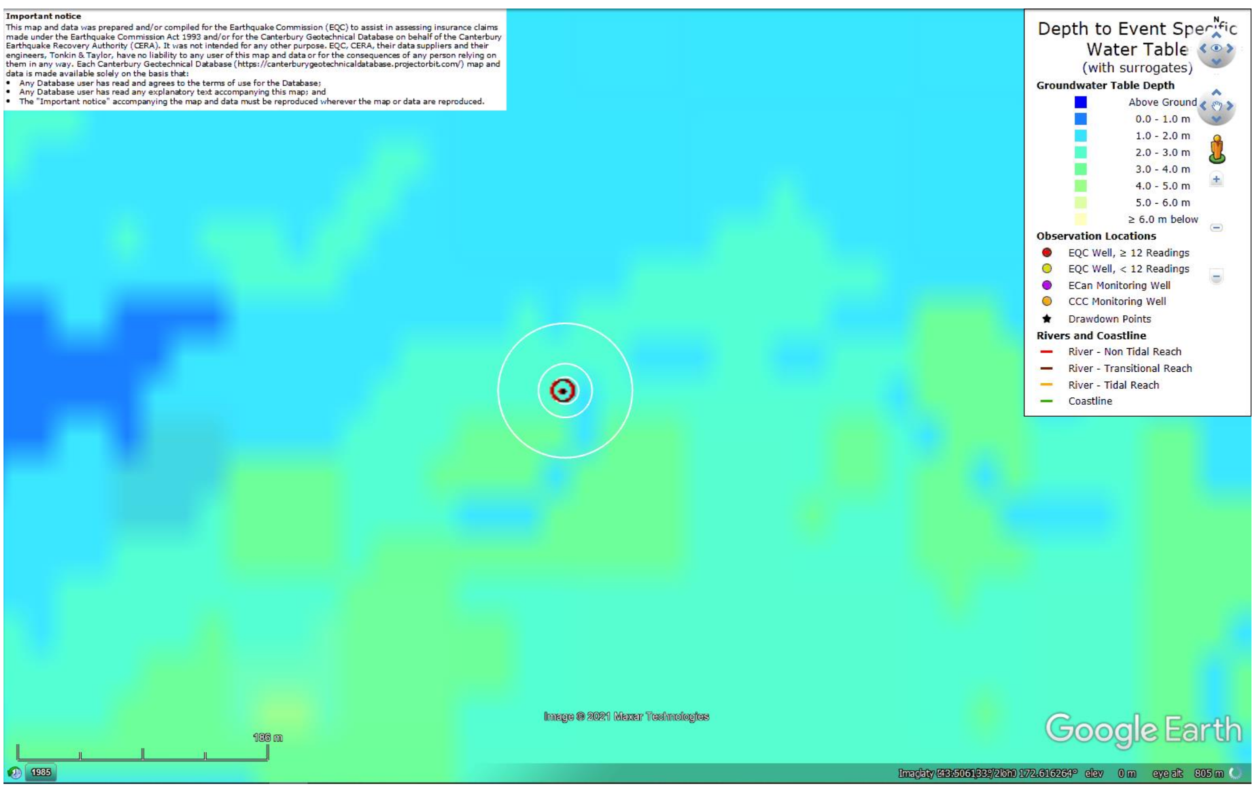

Figure 30: Depth to groundwater table for Sep-10 EQ.

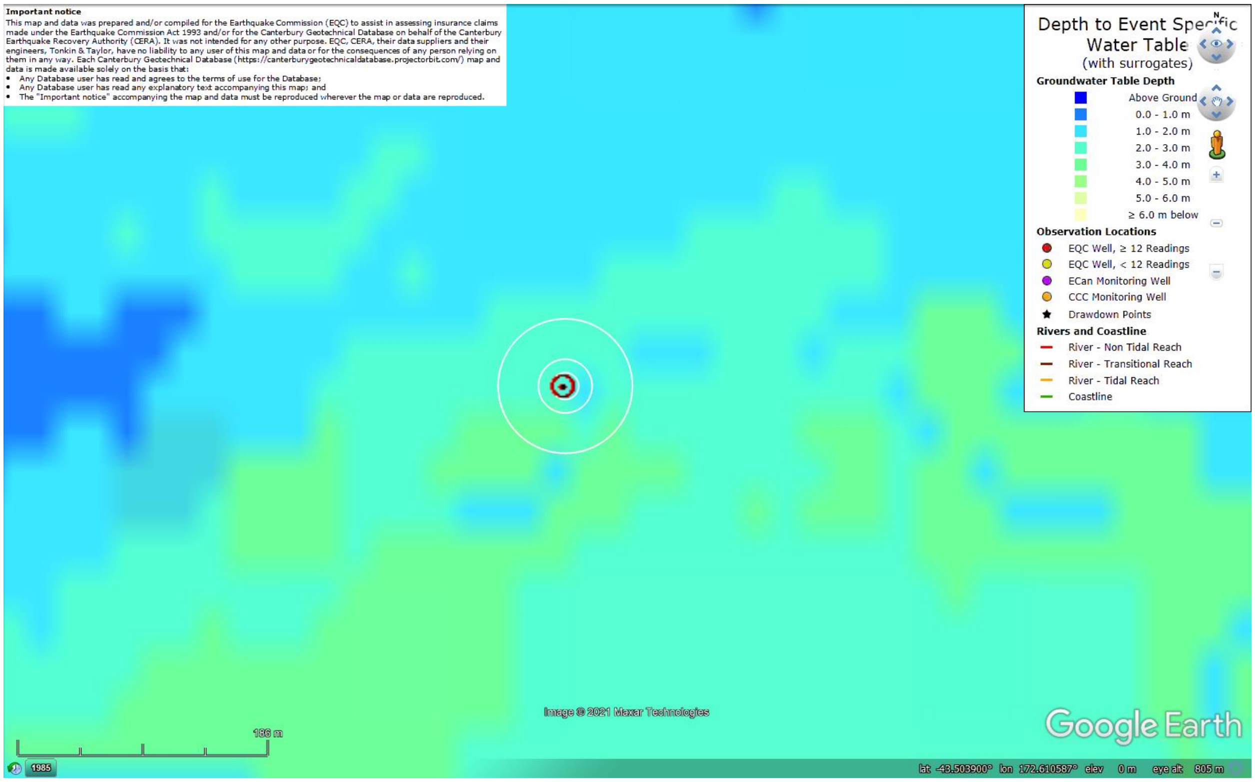

Figure 31: Depth to groundwater table for Feb-11 EQ.

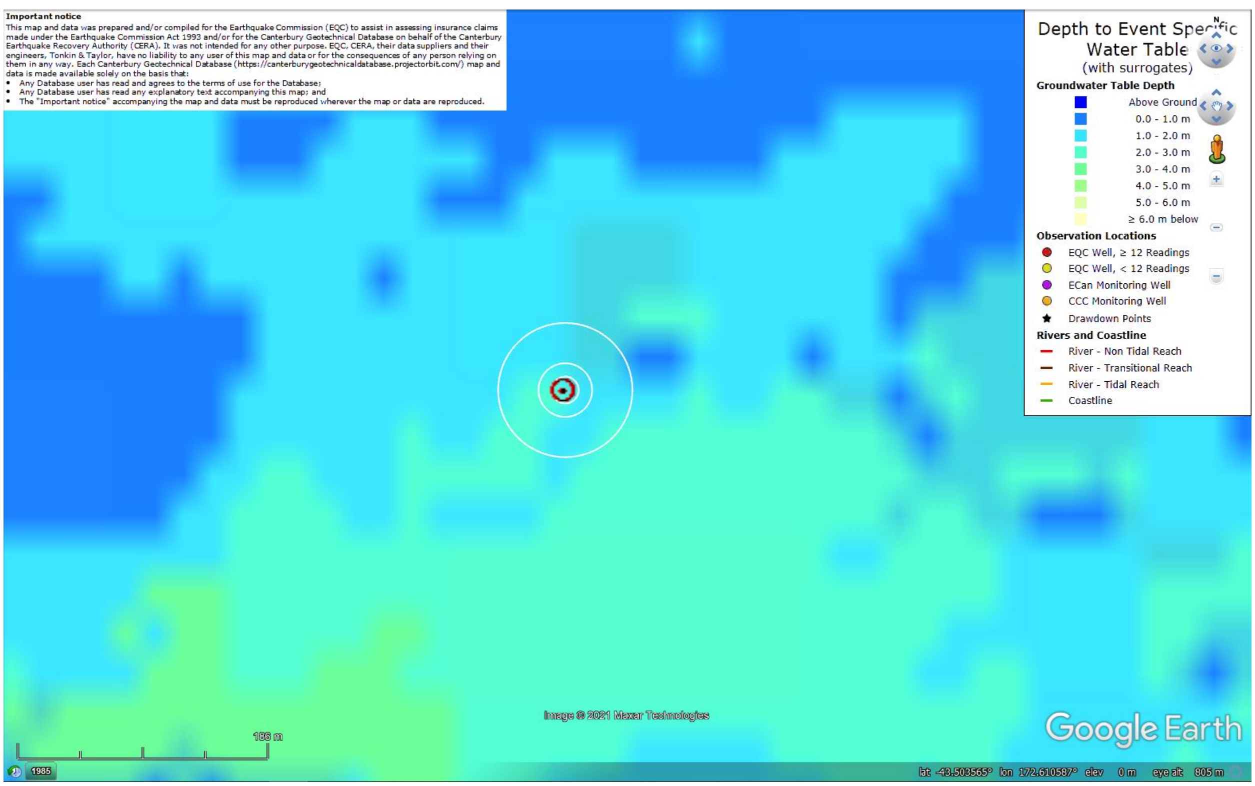

Figure 32: Depth to groundwater table for Jun-11 EQ.

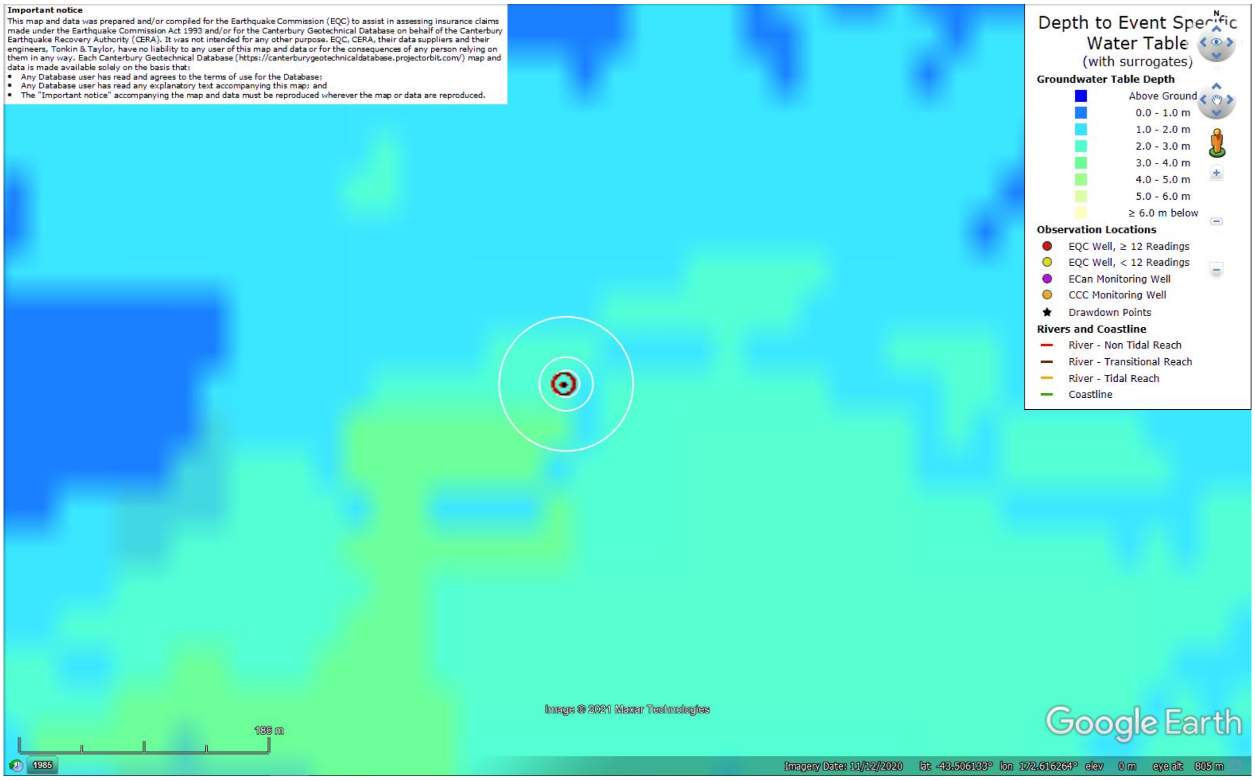

Figure 33: Depth to groundwater table for Dec-11 EQ.

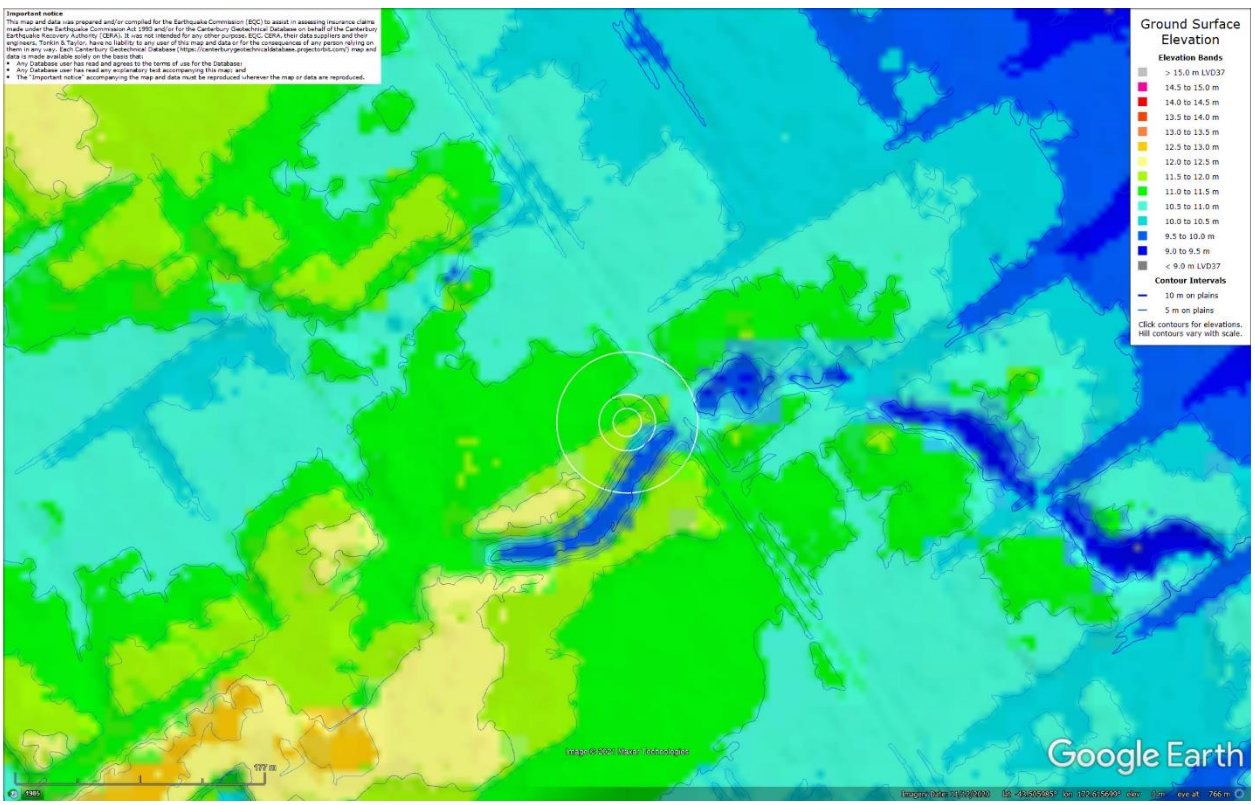

Figure 34: Ground surface elevation according to the Sep-11 LiDAR survey.

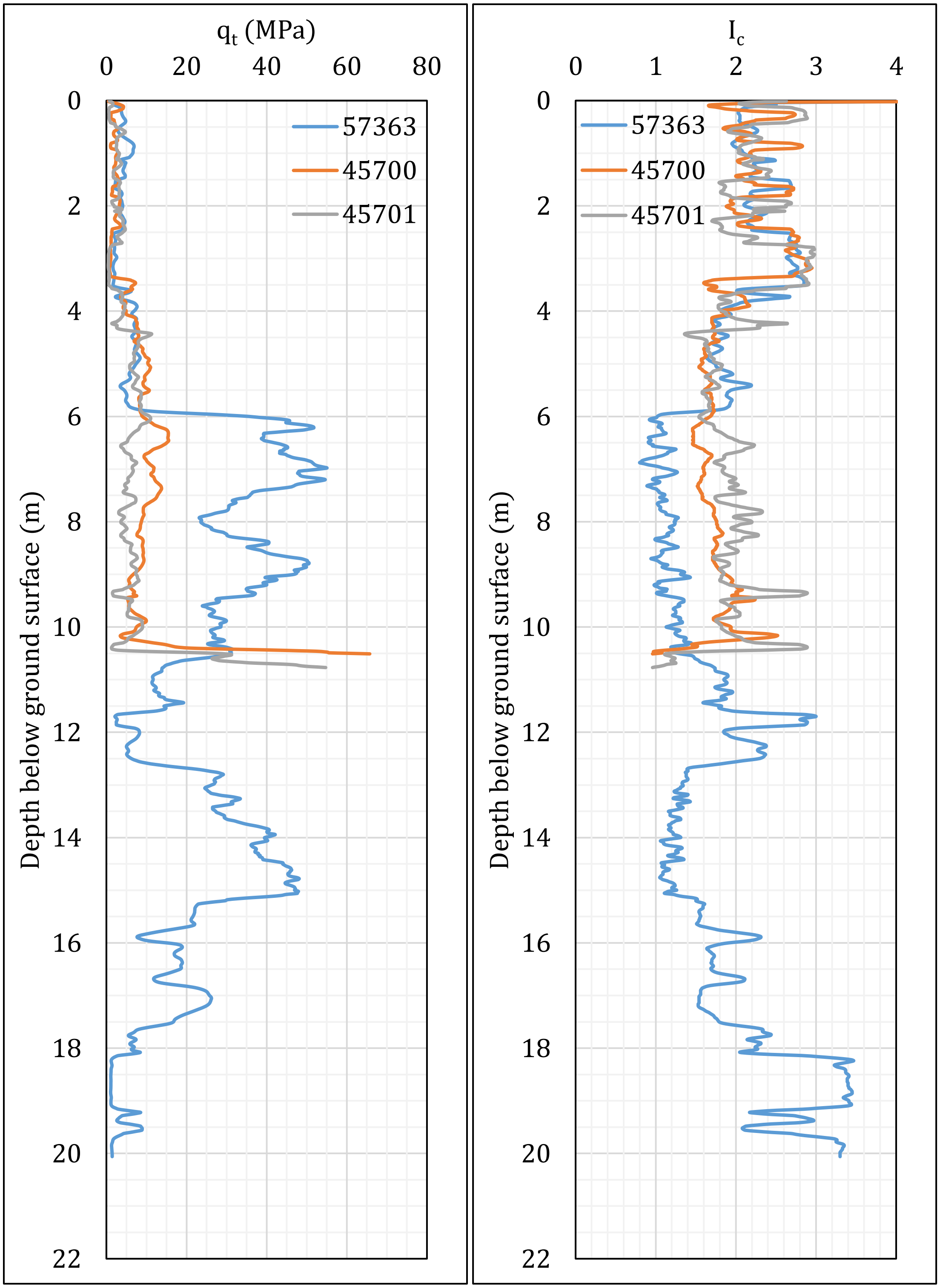

Figure 35: q_t and I_c profiles.

Note 5: The selection of CPTs for the area considered for settlement assessment (Figure 1) is based on the proximity of the CPTs to the considered areas. In accordance with that, the following table shows CPTs that were used for the volumetric settlement analysis in *Cliq v.3.0.3.2*, a CPT soil liquefaction software developed by GeoLogismiki. (The average volumetric settlements were reported in Table 8.)

Table 12: CPT profiles used in volumetric settlement analysis for areas selected for settlement assessment.

CPT ID No.	Road (20-m buffer)	Road (50-m buffer)
57363	✓	✓
45700	✓	✓
45701		✓

Note: CPT 57363 was used to calculate the volumetric settlement for a depth range from 10.52 m and 10.78 m for CPTs 45700 and 45701, respectively.

Table 13: CPT-based results.

		CPT ID			
EQ Event	Parameter	57363	45700	45701	$\Delta_{CPT45700/CPT45701}$
Sep-10	S_{V1D} (mm)	30	45	81	18
	LSN	4	6	12	1
	LPI	0	1	3	0
	LPI_{ish}	0	0	0	--
	$D_{FS<1}$ (m)	5.38	7.67	4.72	--
Feb-11	S_{V1D} (mm)	ND	ND	ND	ND
	LSN	ND	ND	ND	ND
	LPI	ND	ND	ND	ND
	LPI_{ish}	ND	ND	ND	ND
	$D_{FS<1}$ (m)	ND	ND	ND	ND
Jun-11	S_{V1D} (mm)	ND	ND	ND	ND
	LSN	ND	ND	ND	ND
	LPI	ND	ND	ND	ND
	LPI_{ish}	ND	ND	ND	ND
	$D_{FS<1}$ (m)	ND	ND	ND	ND
Dec-11	S_{V1D} (mm)	ND	ND	ND	ND
	LSN	ND	ND	ND	ND
	LPI	ND	ND	ND	ND
	LPI_{ish}	ND	ND	ND	ND
	$D_{FS<1}$ (m)	ND	ND	ND	ND

Notes: $D_{FS<1}$ = Depth to the first liquefiable layer (FS_L<1) that is at least 200-mm thick, as determined by the Boulanger and Idriss (2016) liquefaction-triggering procedure (P_L=50%, C_{FC}=0.13, and $I_{c,cutoff}$ =2.6), and exported from *Cliq v.3.0.3.2*; $\Delta_{CPT45700/CPT45701}$ indicates the amount of SV1D, LSN, and LPI added to CPTs 45700 and 45701 due to the shallow penetration depths.

Note 6: Based on the borehole log (BH 57256, Figure 1), the groundwater table is at a depth of 3.2 m below the ground surface. The soil profile consists of (1) topsoil (organic silt) to a depth of 0.1 m and silty fill to a depth of 0.5 m, (2) silt, ML, to a depth of 4.15 m, (3) silty sand, SM, to a depth of 4.4 m, (4) fine sand, SP, to a depth of 6.35 m, (5) sandy fine to coarse gravel, GW, to a depth of 11.65 m, (6) silt with minor gravel, ML, to a depth of 11.85 m, (7) fine sand, SP, to a depth of 13.15 m, (8) sandy fine to coarse gravel, GW, to a depth of 15.1 m, and (9) fine to coarse sand, SW, to a depth of 15.65 m (the end of the borehole). All soils layers (apart from the topsoil and the fill) are the Yaldhurst members of the Springston formation.